Indian Journal of Chemical Technology
Vol. 29, November 2022, pp. 599-615
DOI: 10.56042/ijct.v29i6.67432

Sonocatalytic degradation of direct blue dye using semiconductor nanocatalyst

R Bhavani & A Sivasamy*

Catalysis Science Laboratory, CSIR-Central Leather Research Institute, Adyar,
Chennai 600 020, Tamil Nadu, India
Email: arumugamsivasamy@yahoo.co.in

Received 19 August 2022; accepted 21 October 2022

The toxic pollutants present in water should be treated by advanced oxidation processes (AOP). This investigation deals with study of sonocatalytic degradation of the prepared zinc oxide nanorods (ZnONR) under ultrasonic (US) irradiation for the degradation of Direct blue (DB71) dye molecule. ZnONR has been prepared by sol-gel method using zinc acetate and ammonia. The prepared ZnONR have been characterized using FT-IR, XRD, FE-SEM, HR-TEM, EDAX, AFM and BET techniques and found that the prepared catalyst is highly crystalline with hexagonal structured nano rods with Wurtzite crystal phase. *In-situ* generation of the $OH^{\cdot}$ radicals has been analyzed by EPR technique. Preliminary experiments are conducted such as effects of *p*H, catalyst loading, dye concentration and effect of energy input to optimize suitable experimental conditions. Kinetics of sonocatalytic degradation of dye molecules have also been carried out and the reaction followed pseudo first-order kinetics. The interference of electrolytes on the degradation of dye molecules has also been carried out. Degradation of the dye molecules are examined by UV-Visible absorption, COD and TOC measurements. The by-products formation of the degraded samples has been analyzed by ESI-MS^{+} technique. The reusability of the catalyst for its efficiency and the degradation of real dye house effluents have also been tested

Keywords: Sonocatalysis, Direct blue, Advanced oxidation, Mineralization, Degradation, Surface area

The Industrial revolution and population growth which results in the rapid development of science and technology, led to the generation of enormous quantities of waste which threaten the natural resources like air, land, soil and water. The removal of toxic contaminants present in the wastewater by using proper techniques, is nowadays challenging to the researchers. Heterogeneous semiconductor catalysts are receiving great consideration by the investigators for the exploitation of its catalytic activities. In the recent years, semiconductor nanomaterials have been used for the degradation of organics and inorganics using Advanced Oxidation Processes (AOP). Different ways of oxidation and/or reduction have been described in the literature elsewhere[1-3].The most relevant method is AOP which play a main role in the oxidation of organics such as the destruction of non-biodegradable organic/ inorganic compounds. Even compounds containing azo dyes which can be mineralized successfully into non-toxic materials by the effective and non-selective chemical oxidant $OH^{\cdot}$ Radicals[4]. Degradation of organics by means of Fenton's reagent[5,6], Ozone[7], semiconductor catalysts like ZnO[8], TiO_2[9] and iron oxide[10]etc., into harmless substances like carbon dioxide and water[11] under photocatalytic and sonocatalytic methods were described elsewhere[12-14].

Ultrasound plays a major role on the degradation of toxic pollutants can increase the catalytic activity of the semiconductor metal oxide catalysts combined with (US) irradiation by the vigorous turbulence produced with required energy input. Which is used for the degradation of organics and inorganics gave good results using Fenton reagent[7], ozone[15], TiO_2[16], and ZnO[17] etc., are broadly described in the literature. ZnO is a best catalyst for the degradation of trace pollutants in water[18]. Additionally combination of US irradiation and influencing effect of zinc oxide nano particles may increase the activity of the catalytic process due to the large surface area, and high catalytic action, low cost and lower toxicity[19-21]. Use of ZnO for the degradation of pollutants under ultrasound is seldom described in the literature[22-24]. So it is worth to examine the catalytic activities of the semiconductor ZnONR catalyst under ultrasonic irradiation for the degradation of organics/inorganics in the aqueous solution.

Ultrasound is a sound wave with a frequency greater than 16-20 kHz. Under ultrasound, cavitation results in the formation, growth and following collapse of micro

cavities (hotspots) producing very high turbulent waves in liquid with very high temperature and pressure releasing large magnitudes of energy over millions of locations in the reactor at once which could increase the reactivity by many fold[25,26]. Here the sound energy is exploited for the generation of very high reactive OH• radicals created from the aqueous phase through cavitation by the destruction of the dye molecule. Degradation of organics is accomplished through a combination of pyrolytic reactions taking place inside or near the bubble and hydroxyl radical-mediated reactions occur in the liquid[27,28].When semiconductor catalyst in the aqueous solution was treated with US, it feels sonolysis of water molecules and also links with the catalyst to give electron-hole pairs in reaction. The electron-hole pairs can produce $OH^{\bullet}$ which can degrade the dyes to CO_2, H_2O and inorganic species[29]. Along with the cavitational effect, the sonoluminescence of US stimulates ZnONR to produce additional OH• through the disintegration of water molecules by holes (h^+). The sonication of water produces hydroxyl radicals in chemical equations as given below[1-8].

$$H_2O\ ))) \rightarrow OH^{\bullet} + H^{\bullet} \quad \ldots (1)$$

$$2OH^{\bullet} + 2H^{\bullet}))) \rightarrow H_2O_2 + H_2 \quad \ldots (2)$$

$$H_2O_2 + \bullet OH \rightarrow H_2O + HO_2^{\bullet} \quad \ldots (3)$$

$$HO_2^{\bullet} + \bullet OH \rightarrow H_2O + O_2 \quad \ldots (4)$$

$$H_2O_2 +))) \rightarrow 2OH \bullet \quad \ldots (5)$$

$$\text{Catalyst} + \text{Ultrasound} \rightarrow e^- + h^+ \quad \ldots (6)$$

$$h^+ + H_2O \rightarrow OH^{\bullet} \quad \ldots (7)$$

$$OH \bullet + \text{Dye}\ ))) \rightarrow CO_2 + H_2O + \text{Oxidation products} \quad \ldots (8)$$

Where,))) means ultrasonic irradiation.

Direct Blue 71 (DB71) is toxic, mutagenic and carcinogenic contaminants in effluents from industries[31]. Direct blue 71 is a tri-azo dye useful to stain membrane-immobilized antibodies, proteins and in adsorption studies. So, it is very important to eradicate these dreadful chemicals from the watercourse through proper treatment processes. Hence, the present study is focused on the preparation and characterization of ZnO nanorods and its catalytic activities on the degradation of DB71 under ultrasound is explained in detail.

Experimental Section

Materials and instrument

DB71 dye (1,5-Naphthalenedisulfonicacid,3-[[4-[[4-[(6-amino-1-hydroxy-3-sulfo-2-naphthalenyl)azo]-6-sulfo-1 naphthalenyl] azo]1naphthalenyl] azo] tetrasodium salt was purchased from Sigma-Aldrich (India) Bangalore, India. 5,5-Dimethyl 1-Pyrroline N-Oxide (DMPO), was purchased from Sigma-Aldrich, USA. Magnesium chloride, silver sulphate, sulphuric acid, hydrochloric acid, sodium hydroxide and potassium hydrogen phthalate were purchased from S.D. Fine Chem., Mumbai, India. Zinc acetate (98% $Zn(O_2CCH_3)_2(H_2O)_2$), Sodium chloride and ammonia were procured from Rankem, Mumbai, India. Potassium dichromate and ammonium ferrous sulphate were supplied by Qualigens, Mumbai, India. Potassium chloride, sodium bicarbonate, sodium chloride, ethanol, buffer tablets were supplied by Merck, Mumbai, India. Dye house effluent was collected from Pilot Tannery, CSIR-Central Leather Research Institute, Chennai, India. All the chemicals are analytical grade and used as received without extra purification. DMPO was purified[32] and processed before analysis.

The prepared ZnO nanoparticles were characterized by FT-IR, XRD, FE-SEM, HR-TEM, AFM, BET and EPR techniques. The functional group of the prepared semiconductor material were characterized by FT-IR spectroscopy using a Perkin-Elmer FT-IR spectrometer. The crystallinity of the prepared semiconductor material was characterized by XRD technique using a PAN analytical X-ray diffractometer, (Germany) with Cu Kα radiation in the 2θ scan range between 10º and 70º, at an accelerating voltage of 40 kV and an emission current of 25 mA. The surface morphology and size of the particles of the sample was analyzed by FE-SEM and EDAX (Model Supra 55 - Carl Zeiss, Germany) and the HR-TEM analysis was carried out in a JEOL 3010 (JEOL Ltd. Japan) instrument. The surface roughness and porosity of the sample was determined by atomic force microscopy technique (Model-NTEGRA PRIMA-NTMDT, Ireland) by using the contact angle mode. The surface area, porosity and distribution of pore size and pore volume of the prepared semiconductor material was analyzed by BET analysis in a Belsorpmini–II instrument (Japan). The *in-situ* formation of $OH^{\cdot}$ free radicals upon ultrasonic irradiation of the ZnO was confirmed by EPR analysis using Bruker, Model EMX X Band, electron paramagnetic resonance spectrometer (Germany). Sonocatalytic experiments were performed using (Sonics, Vibracell, USA,20 kHz, 750 W) horn and split type probes. The sonocatalytic degradation of the dye molecule was monitored by the UV-visible spectrophotometer using the liquid sample holder in UV 2600 (Shimadzu, Japan) spectrometer in a scan

speed of 200 nm/min. The COD analysis was carried out in the (Thermo reactor Spectroquant TR-320, Merck, Germany) block digester. TOC was analyzed using Multi N/C 2100 S BUTOC analyzer (Analytikjena, AG Germany). The by-product formation was also analyzed using Electrospray Ionization Mass spectrometric (ESI-MS+) analysis with positive mode.

Preparation of the catalyst

ZnONR's were prepared by modified Sol-gel process[33,34] using and ammonium hydroxide as a precipitating agent. Prepared 0.2 M Zinc acetate solution by dissolving 10 gm of zinc acetate in 200 ml of double distilled water. The initial *p*H of the zinc acetate solution was increased to pH 8 by adding 25% of aqueous ammonia with vigorous stirring till the formation of white precipitate. Then, the precipitate was filtered and the Zinc hydroxide precipitate was formed. Then transferred to a beaker to make slurry with water. Ammonia was rapidly added and stirred well to raise the pH to 11.5 until a clear solution of ammonium zincate was formed. The solution was aged for 2 days at 65°C to allow the ammonia to evaporate. The white crystalline precipitate was washed many times to remove excess ammonia and impurities, filtered and transferred to a silica crucible. Then, the precipitate was dried at 150°C in a hot air oven for one hour and then calcined at 300°C. The resultant zinc oxide was stored in an airtight container.

Sonocatalytic studies

Sonocatalytic degradation experiments were performed in an ultrasound sonicator with horn type and split probes. The sonochemical reactor consists of a 250 mL jacketed glass reactor fitted with accessories for withdrawing samples. The sonotrode is capable of supplying a maximum power output of 750 W. The experimental procedure for the kinetics measurement (10 ppm of initial dye concentration) is as follows: *eg*., 20 mL of DB 71 dye with required amount of catalyst (500 mg) with 180 mL of water (at neutral *p*H 6.34) was charged in a batch reactor (total volume of 200 mL), was introduced in the sonication bath, thoroughly mixed, then immediately withdrawn 5 mL of the sample for 0 min and ultrasonic irradiation (35% amplitude energy input) was passed through the mixture. 5 mL of the aliquots were withdrawn at regular time intervals (0, 5, 10, 15, 30, 45 min and1 hr and so on) during the experiment. The degraded samples consequently collected were filtered and the filtrate was analysed for the reduction in absorbance by UV-Visible scanning spectrophotometer. The calibration graphs were drawn against dye concentration with optical density of the dye samples. The unknown concentrations of the degraded dye samples were computed from the standard graphs. The final concentrations of the dye samples after degradation were determined from the measurement of the optical density. From this the efficiency of the degradation was calculated using equation (9)

$$\text{Degradation efficiency (\%)} = \frac{Co-Ce}{Co} \times 100 \quad \ldots (9)$$

where, C_o and C_e are the initial and final dye concentrations in the aqueous phase respectively. The aliquots withdrawn from the reaction mixture was also analyzed for COD reduction by closed reflux method.

Results and Discussion

Fourier transformed-infra red spectroscopy

The prepared pristine zinc oxide nanorod (PZnONR) was characterized by FT-IR and the results are shown in Fig. 1(a).

A broad band observed between 430-419 cm^{-1} matches to the Zn–O stretching vibrations. The bands at 3250 and 3500 cm^{-1} corresponds to O–H stretching vibrations of moisture or residual $Zn(OH)_2$ present in the samples. The stability of the PZnONR (after the US irradiations - Used zinc oxide nanorod (UZnONR)) were also characterized by FT-IR analysis. It is observed that it may retain its functionality as pristine sample is given in Fig. 1(b).

X-ray diffraction studies (XRD)

The crystallinity of the PZnONR catalyst was confirmed by X-ray diffraction analysis which gives the information about the phase identification and estimation of the crystallite size of the catalyst. The XRD pattern of the PZnONR is illustrated in Fig. 2.

It is observed that the PZnONR was in a fine crystalline state and gave the diffraction peaks at 2θ = 31.778°, 34.428°, 36.258°, 47.548°, 56.608°, 62.868°, 66.388° and 67.968° which agrees with their miller indices ((100), (002), (101), (102), (110), (103), (200) and (112)) representing that the phase of the ZnONR is in hexagonal (wurtzite) structure. The XRD data are matched with the literature data

(JCPDS Card, No. 36-1451). The crystallite size of the PZnONR was calculated using Debye-Scherrer Equation (10)[35]

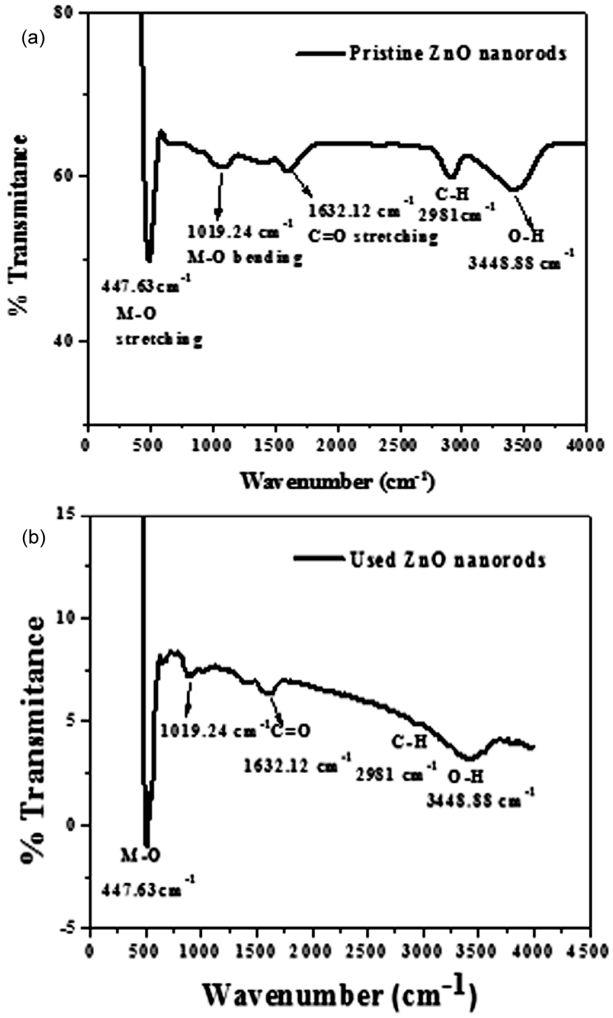

Fig. 1 — (a) FT-IR spectrum of prepared pristine ZnONR and (b) used ZnONR

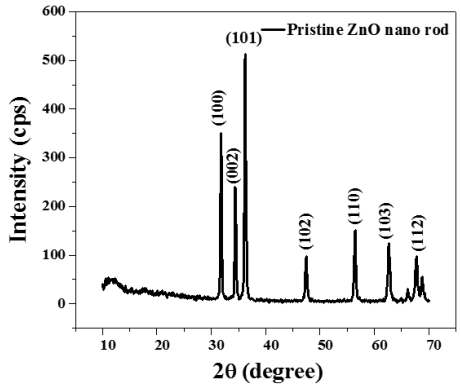

Fig. 2 — XRD pattern of the pristine ZnONR

$$D = \frac{k\lambda}{(\beta \cos \theta)} \quad \ldots (10)$$

where, 0.89 is the Scherrer's constant, λ is the wavelength of X-ray (0.154 nm), θis the Bragg diffraction angle and β is the full width at half-maximum (FWHM) of the diffraction peak. The average crystallite size of the sample was found to be 56.35 nm. The sharp and narrower peaks showed that the ZnONR is in a highly structured and crystalline nature.

Field emission scanning electron microscopy and energy dispersive X-ray diffraction

The surface morphology of the PZnONR was characterized by FE-SEM analysis. The results are shown in Fig. 3.

It is identified that the PZnONR is looked like an independent hexagonal rod-like structure which are scattered in a random manner and all the rods are 88.13 nm equal in size are shown in Fig. 3(a). Elemental composition of the catalyst was determined by EDAX measurement which is given in Fig. 3(b). From the EDAX data, it is established that the prepared material has high purity and contains all the elements like Zn and O in the crystal lattice. For the

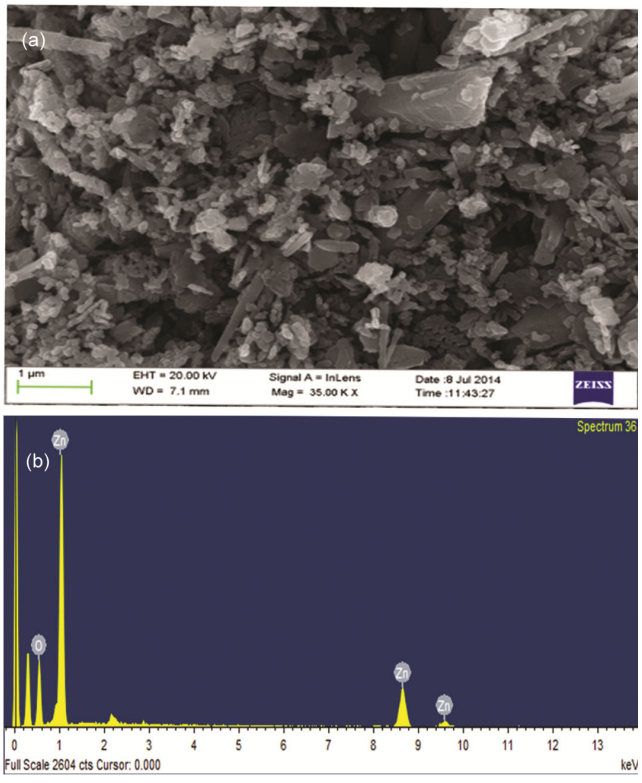

Fig. 3 — (a) FE-SEM micrographs and (b) EDAX analysis of the PZnONR

pristine catalyst a peak at 1 and 8.6 keV indicates the presence of ZnO peaks which reveals that the major portion of the catalyst contains zinc (66.90 wt% and 33.10 atomic%) and tiny peak at 0.5 keV shows the presence of oxide (33.10 wt% and 66.90 atomic%) zoomed at 4 µm. The FE-SEM with EDAX data indicated that there are absence of other metals in the crystal which was established that the catalyst is very pure ZnONR nanostructures.

High-Resolution Transmission Electron Microscopy

PZnONR was analysed by HR-TEM and the image give the information that independent nano rods are placed in random manner as demonstrated in Fig. 4(a).

From the HR-TEM with EDAX data the PZnONR showed a peak at 1 and 8.6 keV displays the existence of ZnO and major part of the sample contains zinc (75.61wt% and 43.13 atomic %). The small peak at 0.5 keV shows the amount of oxygen present (24.38 wt% and 56.86 atomic %) as shown in Fig. 4(b). A peak shows the presence of Cu and this arises from the copper grid which was used in the instrument during the analysis. The Selected Area Electron Diffraction (SAED) pattern of PZnONR shows that the atoms are all arranged in circular mode in a crystal lattice is shown in Fig. 4(c).

Atomic Force Microscopy

The AFM images of the PZnONR in Figs 5(a) and (b) shows the surface roughness and porosity.

It is witnessed that the average roughness is found to be 44.42 nm in the scan area of 3×3 µm. The apex portion of the nano rods are all filled in such a manner which gave a spherical shape. The cross sectional line profile at 164nm of PZnONR is pointed out in Fig. 5(c).

Surface area analysis by BET method

The BET specific surface area of the pristine and used ZnONR were analysed by BET method (nitrogen multilayer adsorption measurement) as a function of relative pressure. The technique is used to calculate the external surface area and pore area for the determination of the total specific surface area in m^2/g. The N_2 adsorption and desorption isotherm of the PZnONR and used ZnONR are shown in Fig. 6 and Table 1.

The pore volume of PZnONR was found to be $9.8 \times 10^{-3} cm^3/g$, pore area $4.81 m^2/g$ and pore diameter 7.03 Å and these were calculated using BJH method. The surface area of the used ZnONR is marginally higher compared to PZnONR this may be because of the cavitational effect which lead to structural and morphological changes on the catalyst during the process of dye degradation. Hence, the used ZnONR was also characterized by FTIR, FE-SEM and HR-TEM techniques.

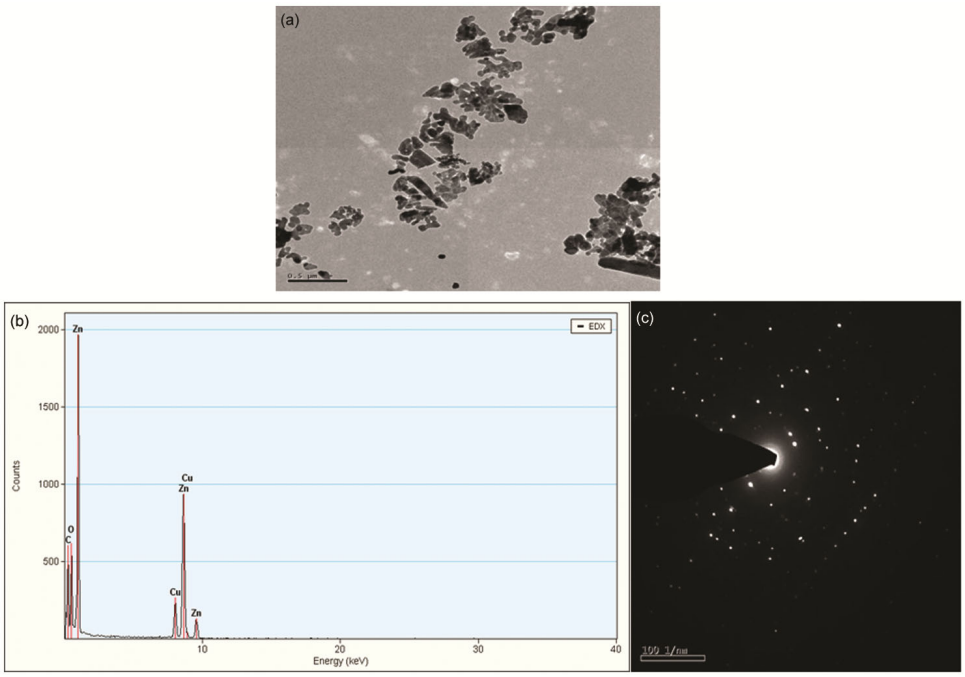

Fig. 4 — (a) HR-TEM micrographs; (b) EDAX analysis and (c) SAED pattern of the PZnONR

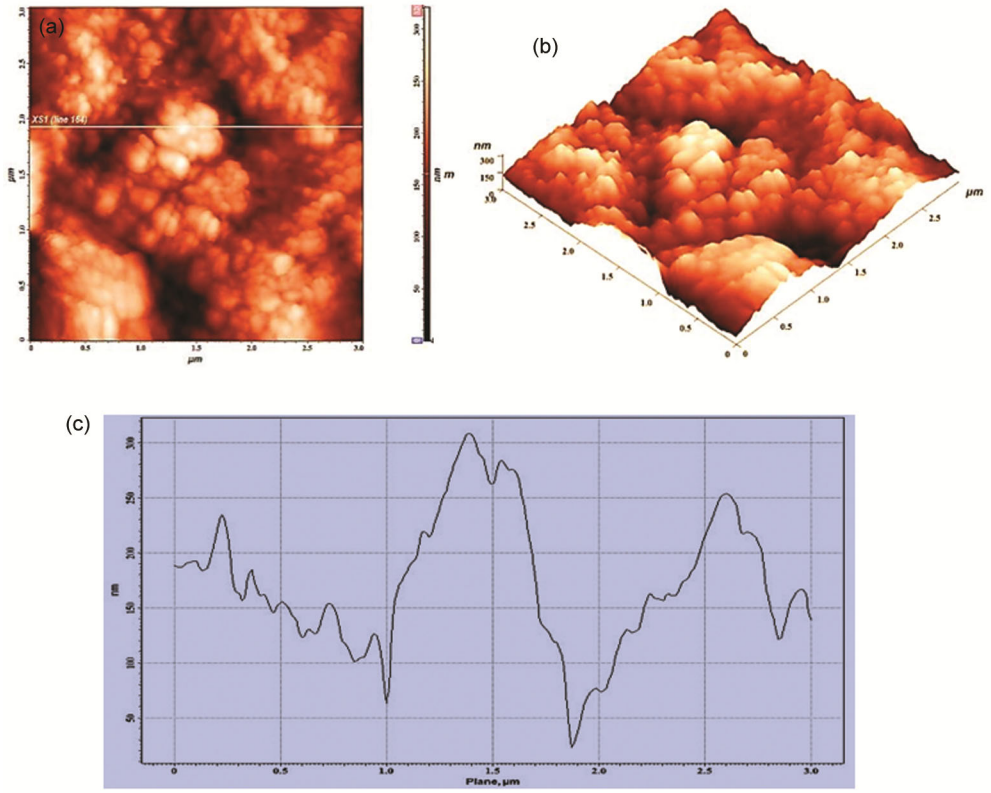

Fig. 5 — Atomic Force Microscopic analysis, (a) 2 D; (b) 3 D images and (c) Surface roughness profile of PZnONR

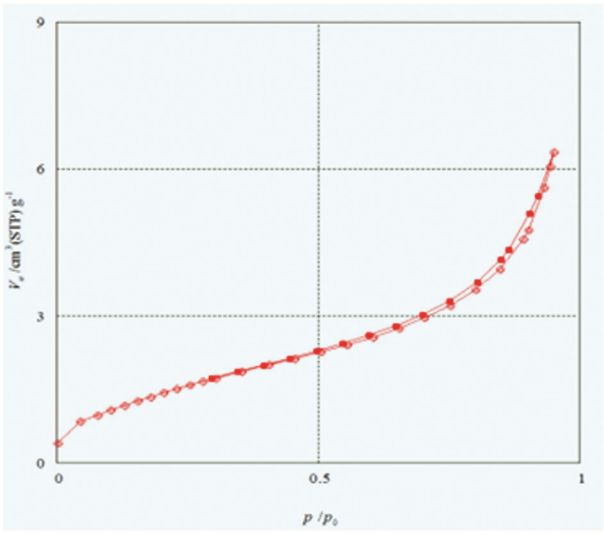

Fig. 6 — N_2 adsorption – desorption isotherm for the determination of surface area of pristine ZnONR

Characterization of the used ZNONR catalyst

FTIR analysis

The FTIR analysis of used ZnONR shows that there is no change in the FT-IR spectra for both the pristine and used ZnONR catalysts. This indicates that the functionalities of the ZnONR are remain unchanged even after the sonication. This is confirmed from the Fig. 1(b)

Table 1 — BET surface area, total pore volume and BJH pore diameter of pristine and used ZnONR

Sample ZnONR	BET surface area (m^2/g)	Total pore volume ($\times10^{-3}cm^3/g$)	BJH Pore diameter (Å)
Pristine	5.57	9.8	7.03
Used	8.20	20.9	10.2

FE-SEM and EDAX analysis of used ZnONR

The morphology of the used catalyst was studied by FE-SEM and the images are shown in Fig. 7(a).

The used ZnONRs were well arranged like a dandelion flower as shown in Fig. 7(a). Particle size of the Pristine and used ZnONR are found to be 88.13 nm and 44.44 nm correspondingly. From FE-SEM analysis that the particle size was found to be reduced when compared to PZnONR. The microscopic analysis of the pristine and used catalysts shows that the surface of the catalyst remains as clean, because during the oxidation of dye molecules, the by products are removed simultaneously along with surface oxide coatings on the surface of the ZnONR. This is because of the turbulence and agitation by

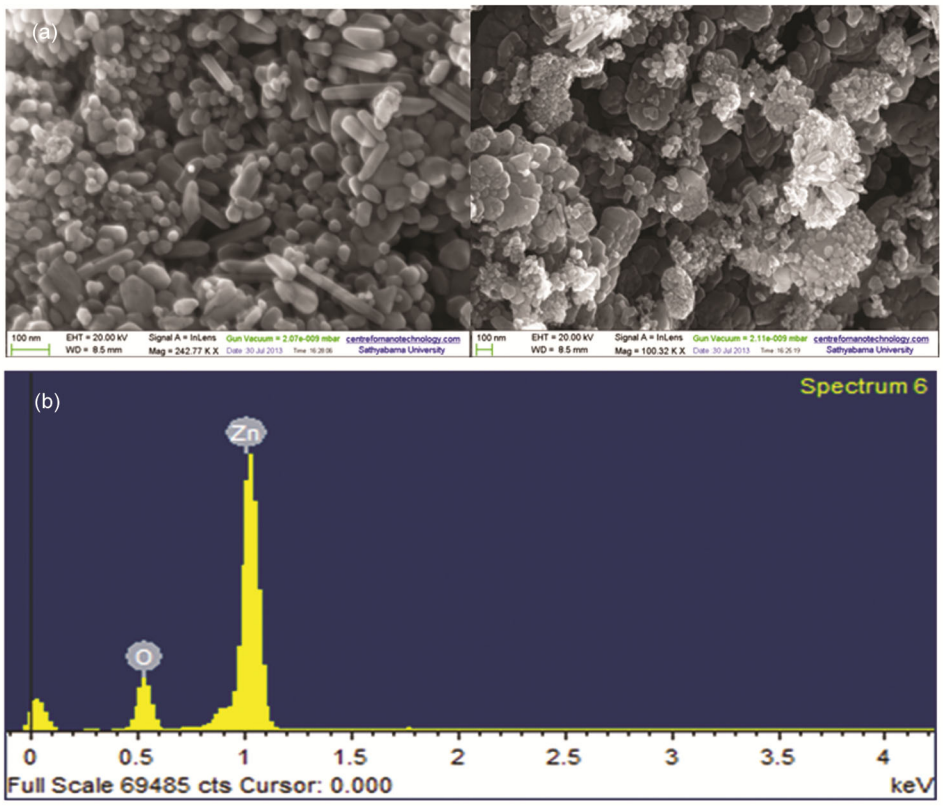

Fig. 7 — (a) FE-SEM micrographs and (b) EDAX analysis of the used ZnONR

cavitational process through ultrasound in the aqueous solution. In addition to this, the continuous impact of the ultrasonic irradiation on the catalyst surface may help to stop the cluster formation of the scattered ZnONRs during catalytic action in the dye degradation process. The used ZnONR after the sonication process shows better stability, surface and morphological characteristics which may improve the catalytic activity in the reusability process. EDAX spectra (from FE-SEM analysis) of used ZnONR catalyst shows that 1keV (72.13 wt% ie., 38.78 atomic %) resembles that main portion of the catalyst has zinc. Then the shorter peak at 0.5 keV shows oxygen at 1 µm (27.87 wt% ie., 61.22 atomic%) which is given in Fig. 7(b).

HR-TEM with EDAX analysis of used ZnONR

HR-TEM micrographs for used ZnONR catalyst are shown in Fig. 8(a). It is observed that the individual nano rods are in an irregular arrangement whereas the used catalyst shows the self-assemblage of the nano rods like a dandelion flowers with cavities inside.

The HR-TEM, EDAX data gives the information that the used ZnONR catalyst shows the presence of ZnO peaks and foremost portion of the catalyst contains zinc (49.00 atomic wt% and 19.31 atomic wt %) and small peak at 0.5 keV shows the existence of oxide (13.68 wt% and 22.05 atomic wt %) as shown in Fig. 8(b). The SAED pattern is shown in Fig. 8(c) which reveals that the used catalyst has the definite systematic and unidirectional arrangement of the atoms in the crystal lattice.

AFM analysis of used ZnONR

The AFM images of the used ZnONR has the average roughness of 25.27 nm like packed arrays (3 D and 2 D image respectively) as shown in Fig. 9 (a) and (b).

The head portion of the nanorods specifies that all are arranged in such a manner to give rod shaped structure. The average roughness of the used ZnONR is lower compared to PZnONR. This is because the surface morphology of the catalyst has changed due to the more ordered nature of the catalyst, so that the roughness has decreased during sonication. Cross sectional line profile of the used ZnONR catalyst at 890 nm shows that the top and bottom portion of the surface of the catalyst as shown in Fig. 9(c).

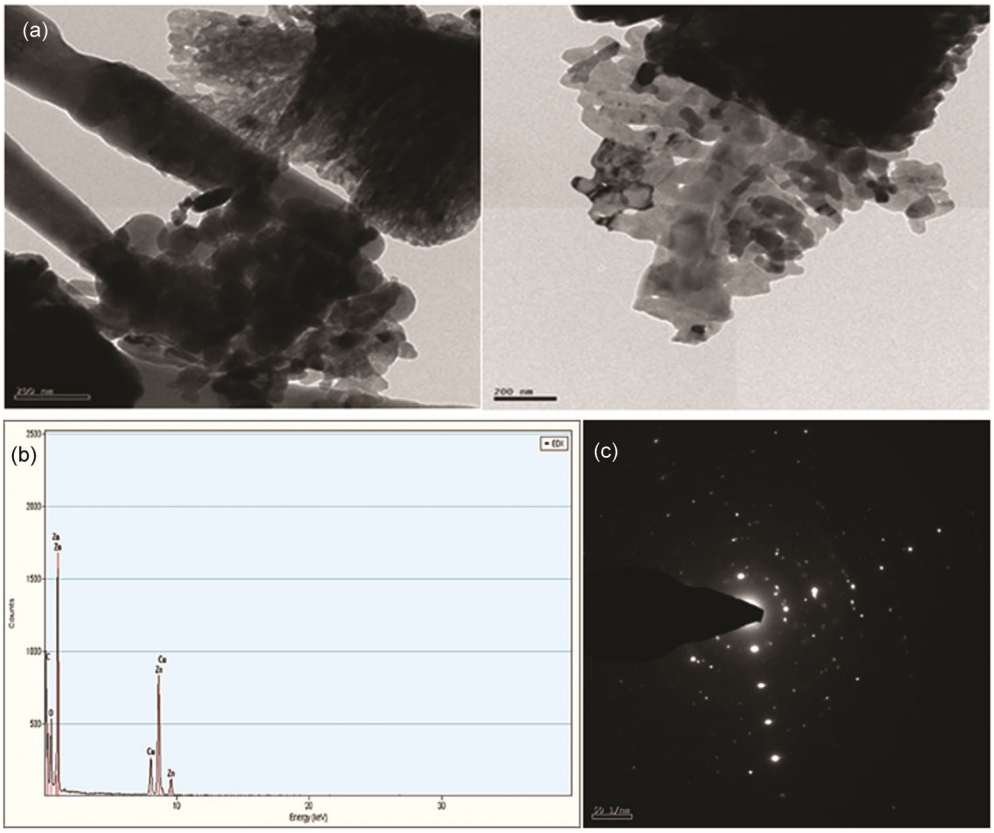

Fig. 8 — (a) HR-TEM micrographs, (b) EDAX analysis and (c) SAED pattern of the used ZnONR

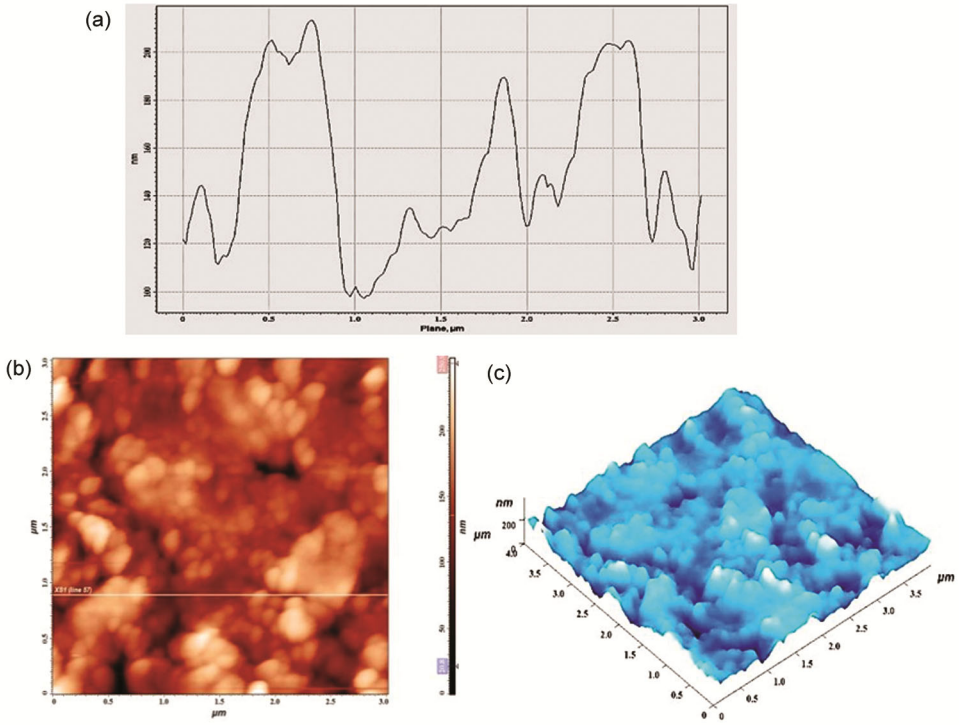

Fig. 9 — Atomic Force Microscopic analysis, (a) 2 D; (b) 3 D images and (c) Surface roughness profile of used ZnONR

Surface area analysis of used ZnONR

The specific surface area of the used ZnONR catalyst is found to be 8.20 m^2/g with pore volume of 1.97 m^3/g, pore area of 6.96 m^2/g and pore diameter 1.96 nm respectively is given in Table 1and Fig. 10(a) and (b).

The BET results illustrates that the specific surface area is somewhat reduced for the PZnONR catalyst but for the used ZnONR the surface area is improved to some extent due to cavitation effect. This may be due to the mechanical shear forces caused by cavitational jet streams by the ultrasound that leads to the particle size and the total surface area of the phase boundary increases simultaneously. Used ZnONR has improved surface properties when compared to pristine catalyst.

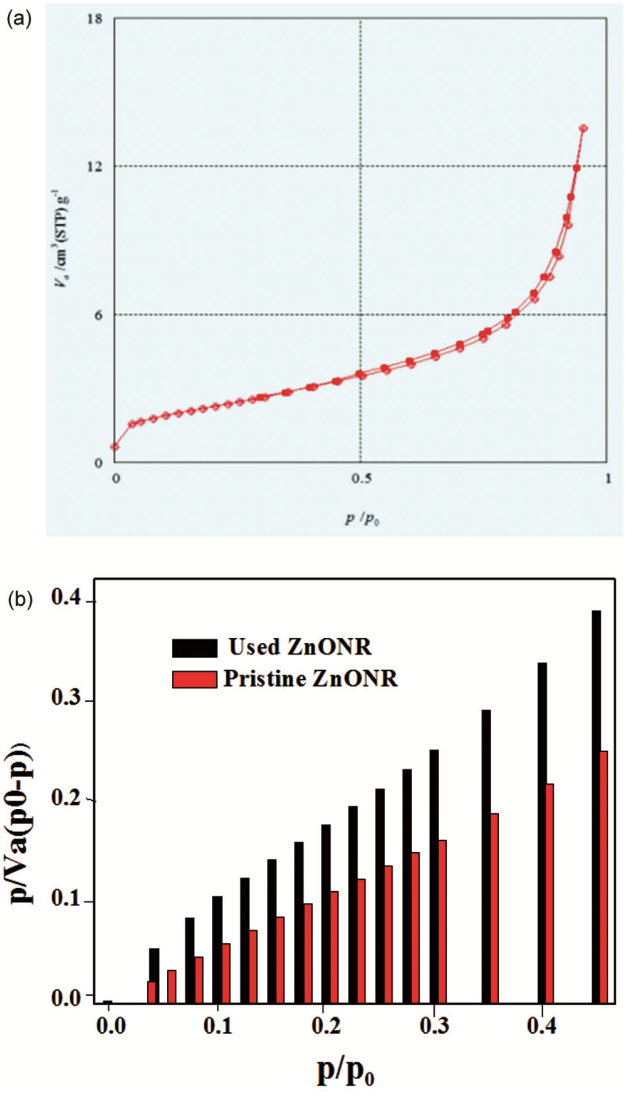

Fig. 10 — N_2 adsorption – desorption isotherm for the determination of surface area of (a) Pristine and (b) used ZnONR

Analysis of in-situ formation of OH radicals by Electron Paramagnetic Resonance spectroscopy (EPR)

The in-situ production of reactive $OH^{\bullet}$ radicals by PZnONR was determined by EPR radical spin trapping technique and DMPO is used as a radical trapping reagent. Accurately weighed 0.125 mg of ZnONR, 40 µL of DMPO and 260 µL of millipore water (300 µL) were taken in an eppendorf tube. The mixture was irradiated in the sonicator for about 5 min at 35% amplitude. Then the mixture was centrifuged at 5000 rpm for 10 min and the EPR spectrum was recorded and analyzed. The experimental result is shown in Fig. 11.

It is noted that the EPR spectrum shows a strong and stable four peak with intensity ratio 1:2:2:1 agreeing with the G values of 3443, 3457, 3472 and 3487 which confirms the presence of OH• radicals. The distance between the two peaks appeared at the center is 15G and 5G for the peaks at the end. These radicals are generated in the in-situ process formed through hot spot mechanism under ultrasonic irradiation in the presence of ZnONRs.

Preliminary studies

Preliminary studies were conducted in order to find out ideal experimental conditions for instance, effects of initial aqueous phase pH, catalyst dosage and the initial dye concentrations for the degradation of DB71 dye molecule under ultrasonic irradiations as shown in Fig. 12.

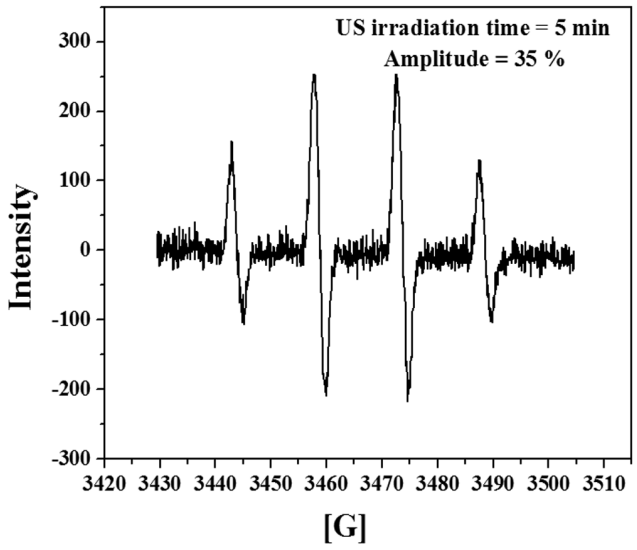

Fig. 11 — EPR spectrum of DMPO spin trapped $OH^{\bullet}$ radicals under ultrasonic irradiation of ZnONR

Effect of aqueous phase *p*H on catalytic activity

The effect of *p*H on sonocatalytic degradation of DB71 was carried out with split probe to find out the optimum *p*H for the degradation process. The maximum percentage degradation was observed at neutral *p*H and it was selected for further experiments. During the US irradiations the positively charged dye molecules can enter into cavitation bubbles, via the hot spot mechanism which indicates the increased degradation efficiency of azo dyes at the acidic range of *p*H as shown in Fig. 12(a). The same phenomena have previously been stated elsewhere[36].

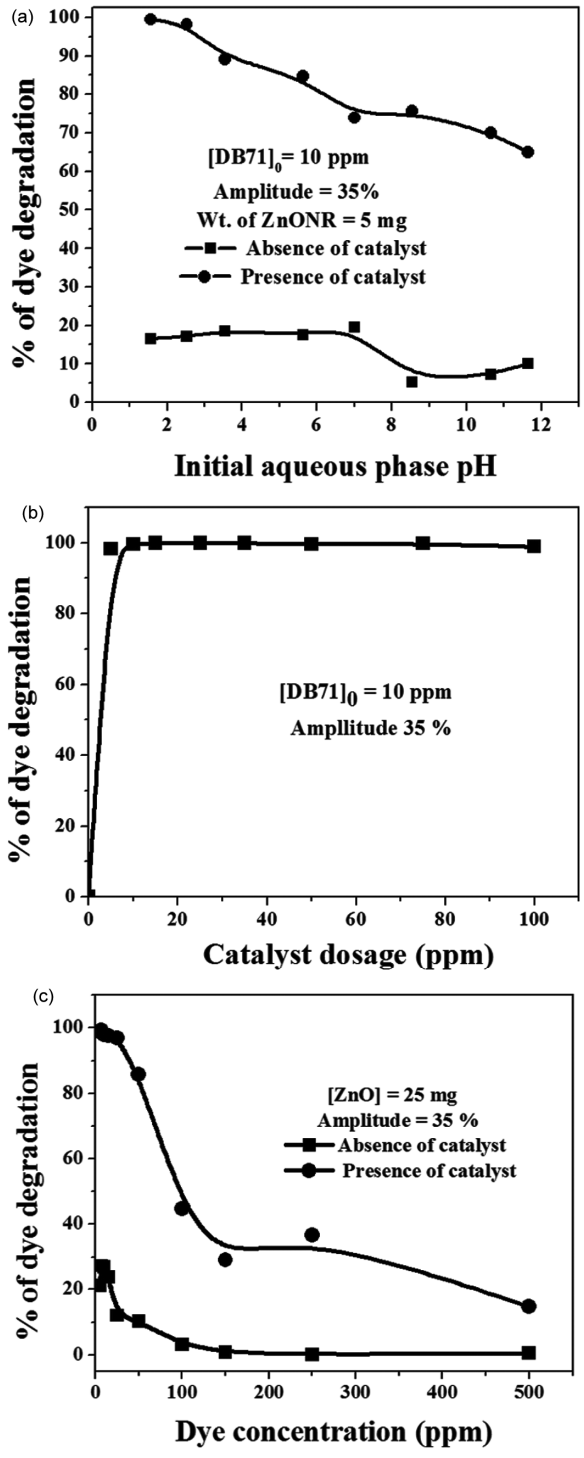

Fig. 12 — Effects of (a) aqueous phase pH (b) catalyst dosage (c) dye concentration on degradation of DB71dye molecule by ZnONR under ultrasonic irradiation

In the *p*H range from 1 to 7, the dye molecules may exist in the form of positive charges. OH^- ions are more at alkaline *p*H, these ions can couple with the holes to form $OH^•$ radicals, these radicals are responsible for the dye degradation. As the *p*H of the solution is increased, the rate of degradation of dye decreases, where more OH^- ions may be available and these ions are adsorbed on the surface of semiconductor making it negatively charged. As a result a decrease in the rate of degradation due to repulsive force between two negatively charged species the movement of the dye molecule to the semiconductor surface will be retarded. These results have also been confirmed with literature[37,38]. The effect of ultrasound on the degradation of dyes in the absence of catalyst it shows that there is a very minimum percentage of degradation followed as shown in Fig. 12(a). This may be due to the cavitation of aqueous phase that creates lesser concentration of $OH^•$ which is responsible for lower % of dye degradation.

Variation of catalyst dosage

The effect of catalyst loading on the maximum degradation of dye molecule under ultrasonic irradiation with ZnONR was studied with optimized *p*H of 6.34 and the dye concentration of 10 ppm and the catalyst loading was varied from 25 mg/10 mL is given in Fig. 12(b).It was detected that the percentage degradation of the dye molecule was increased with increasing catalyst dosage. The maximum degradation followed upto 98% for 5 mg of catalyst dosage. The % degradation decreases marginally after 50 mg of the catalyst dosage. This may be due to the fact that, higher loading of catalyst may lead to the agglomeration of the catalyst in the aqueous phase and further the available surface area may be lesser for the adsorption of dye molecules onto the catalyst surface which further inhibits the catalytic activity[39].

Variation of initial dye concentration

The effect of initial dye concentration on the degree of degradation of dye molecules with

optimized dosage of catalyst is shown in Fig. 12(c). The dye concentrations were varied from 5 to 500 ppm with the catalyst dosage of 25 mg /10 mL at 35% amplitude energy input. The % degradation decreases on increasing the dye concentration in the aqueous phase. The same experiment was carried out in the absence of catalyst. It was noticed that there is low % degradation (21.13 %) was observed.

Effect of energy input dosage

In order to find out the ideal US energy input essential for the maximum dye degradation with different energy inputs such as 25, 35 and 45% amp were conducted in a batch reactor. Because heterogeneous catalytic reactions generally is dependent upon mass transfer of the reactant from bulk solution to catalytic surface, hence an increase in ultrasonic power density will increase mixing intensity due to the turbulence made by cavitation process. The energy input kinetics experimental results shows that 20 min (99.63%), 17 min (99.26%) and 15 min (99.07%) of degradation was achieved (Fig. 13 and Table 2) for all the 25, 35 and 45% amplitude of energy inputs respectively with corresponding time and % degradation.

COD for energy input kinetics experiment for various energy densities like 25, 35 and 45% amplitudes were shown in Fig. 13(b).The decrease of COD level progressed at a more rapidly during the first 30 min of reaction then the % degradation was found to be slower. It is observed that the rate of dye degradation rises correspondingly with increasing the energy input. The kinetic data are analyzed by using the pseudo-first order rate equation.

It can be observed that rate constants are varied from 79.42, 112.30 and 161.41 × $10^{-3}$$min^{-1}$. The R^2 values are found to be above 0.99 as shown in Table 2 and Fig.13(c).

The kinetics for the energy input indicated that the degradation is faster rate at 45% amp when compared to the degradation occurred in 25% and 35% energy densities. Still at 45% amplitude energy input degradation proves slightly lower percentage but the interval of ultrasonic irradiation was substantially reduced compared to 25% amplitude and with 45% amplitude it is slightly higher with higher heat and mass transfer. Considering cost effectiveness 35% amplitude was chosen for the kinetics experiment. This is because the cavitation erosion on particle surfaces produces highly reactive surfaces created short-lived high temperatures and pressures contribute to molecular decomposition and increase the reactivity of many chemical species. In the case of 35% amplitude it can create moderate and constant

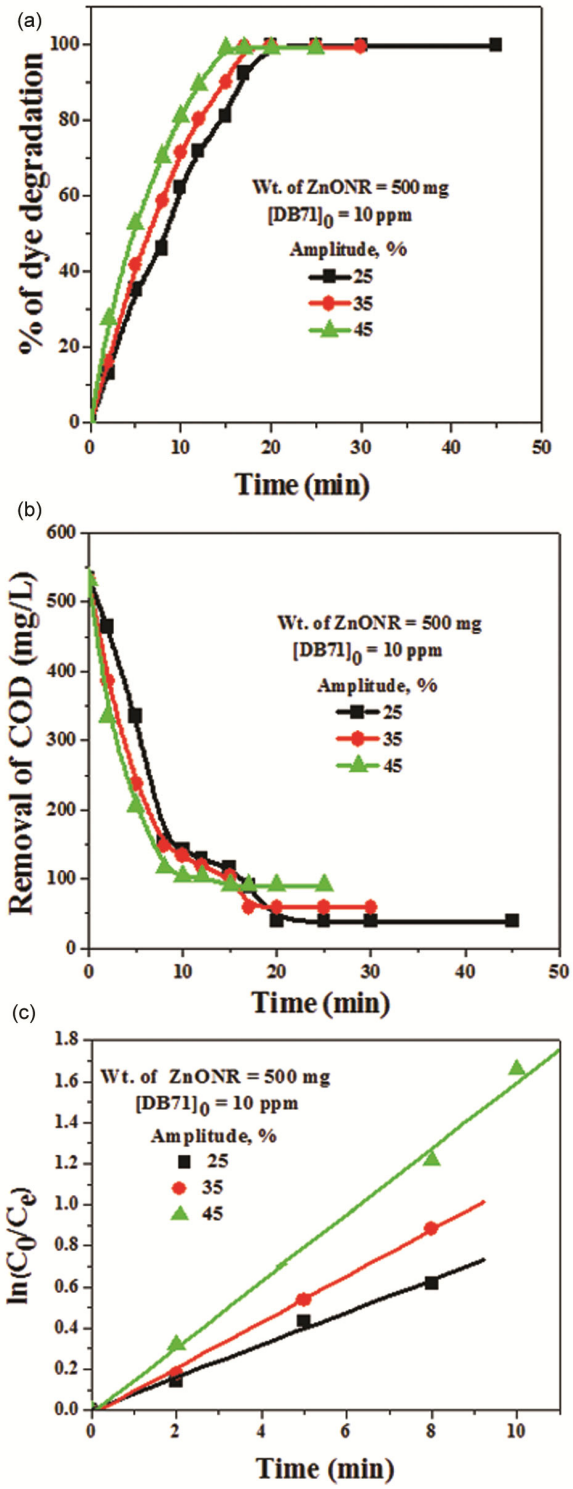

Fig. 13 — Effect of ultrasonic energy input on degradation of DB71 dye molecules (a) % of dye degradation (b) Removal of COD and (c) Pseudo-first order kinetic plots

Table 2 — Pseudo first order rate constants for the sonocatalytic degradation kinetics of DB71 dye molecules

Concentration of the dye molecules (ppm)	Rate constant $\times 10^{-3}$ min^{-1}	R^2
5	188.99	0.997
10	132.47	0.9927
15	86.32	0.9813
20	62.79	0.9647

production of active sites so that 35% amp energy dosage was chosen for the kinetics experiment.

Kinetics of dye degradation

The kinetics of the sonocatalytic degradation of an azo DB71dye molecule was planned to conduct by changing the initial dye concentrations from 5 to 20 ppm in a batch reactor with enhanced experimental conditions using ZnONR catalyst under ultrasonic irradiation at 35% amplitude energy input and the results are shown in Fig. 14.

From the results it was found that 15 (99.26%), 17 (99.26%) and 17 (98.52%) and 20 (98.15) % of degradation was attained for the 5 to 20 ppm of initial dye concentrations respectively as shown in Fig. 14(a). The results showed that the dye molecule was readily degraded. During the degradation, 5 mL of the aliquots were withdrawn from the mixture and COD level was monitored as a function of time during the degradation of dye molecule for all the initial dye concentrations of 5, 10, 15 and 20 ppm and the results are shown in Fig.14(b). From the COD values it was seen that the level of COD decreased from 459.26 to 59.26, 533.34 to 59.26, 607.41 to 103.70 755.56 to 133.33 mg/L for 5 to 20 ppm of initial dye concentration respectively. The kinetics of dye degradation has also been analyzed by recording the optical densities during degradation processes. All the kinetic experiments showed pseudo first order rate constant are shown in Fig. 14(C). The reaction rate constant decreases with increasing dye concentrations for 5 to 20 ppm of initial dye concentrations as given in Table 2.

The prepared ZnO nano catalyst was proved to be having superior sonocatalytic action as observed from the kinetic experiments. The kinetic measurements such as 5 to 20 ppm of dye concentrations shows more than 98% degradation. The results demonstrated that the dye molecule was almost completely degraded. The removal of colour may be due to the synergetic effect of ultrasound assisted catalyst during the dye degradation processes. These results confirm

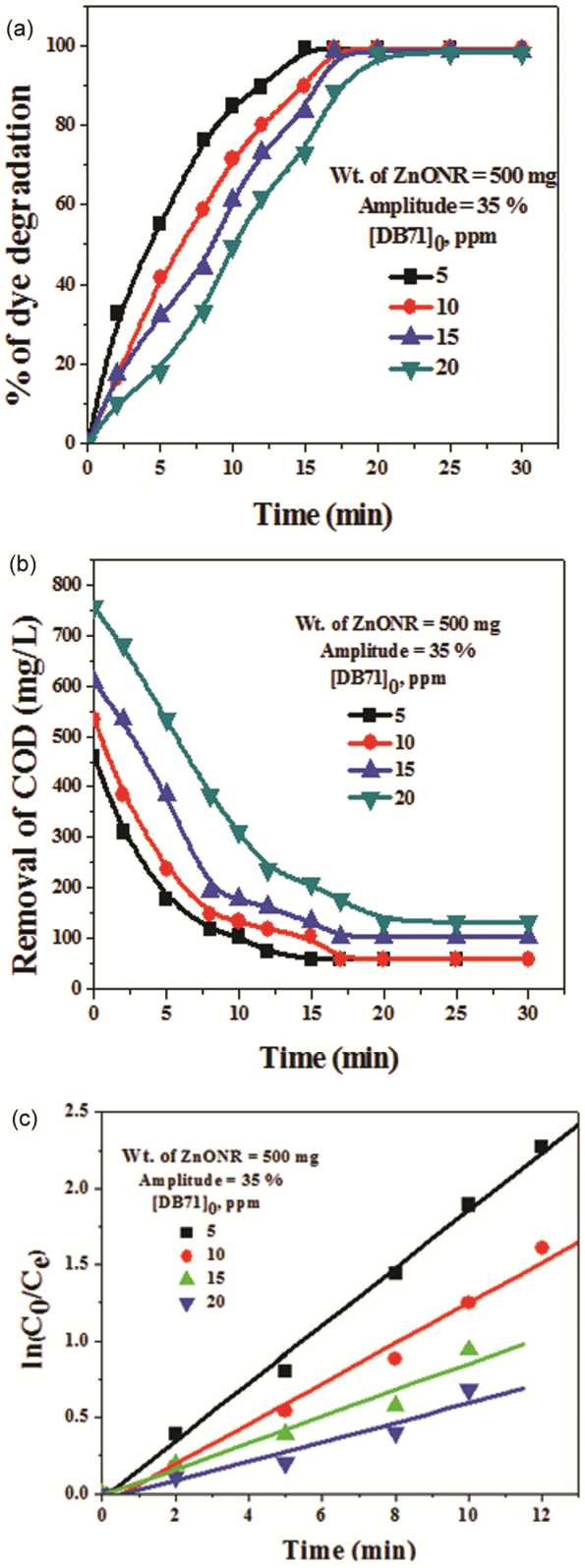

Fig.14 — Kinetics of degradation of DB71 dye molecules using ZnONR under ultrasonic irradiation (a) % of degradation; (b) Removal of COD and (c) Pseudo-first order kinetic plots

that the dye molecules were not only experienced decolorization but may be completely mineralized.

Total Organic Carbon (TOC) analysis

The sonocatalytic degradation of the dye molecules has also been observed by TOC analysis under identical experimental conditions and calculated by the following Equation. (11),

$$\text{Total Organic Carbon} = \frac{TOC_{(ori)} - TOC_{(deg)}}{TOC_{(ori)}} \times 100 \quad \ldots (11)$$

TheTOC of the degraded dye samples were shown in Fig. 15.

From the kinetic study TOC level falls from 117.36 to 33.38 mg/L with 360 min of US irradiation in the presence of ZnONR catalyst. It is noted that TOC level was increased during the course of the reaction.

Effect of electrolytes on dye degradation

Dye house effluents contain number of electrolytes that may inhibit with the degradation process and activity of the catalysts this is because theelectrolytes dissolved through various operations in the industrial dye bath effluent. By varying the concentration of electrolytes from 0.5-5 wt % and all other experimental parameters were kept constant. Added suitable quantity of an electrolyte with dye (10 ppm) and the catalyst (5 mg). Hence, the investigations on the effect of dissolved electrolytes such as NaCl, KCl, Na_2CO_3, $NaHCO_3$, and $MgSO_4$ on the degradation of dye molecules has been studied and the results are shown in Fig. 16.

The addition of sulphate electrolyte rises the % degradation with increasing the electrolyte concentration. This may be due to the formation of $SO_4^{\bullet}$ radicals in the system upon US irradiation during degradation and consequently the SO_4 radicals may improve the degradation processes in addition to OH radicals. But overall efficiency of the degradation was decreased in the presence of chloride, CO_3 and HCO_3 electrolytes.

Mechanism for the catalytic degradation of DB71 dye molecule

The sonocatalytic degradation of dye molecules generally continues through $OH^{\cdot}$ radical mediated process under US irradiations with ZnONR. The effect of US on semiconductor surface and order of reactions occurring in the aqueous phase due to the cavitation process are given in chemical equations

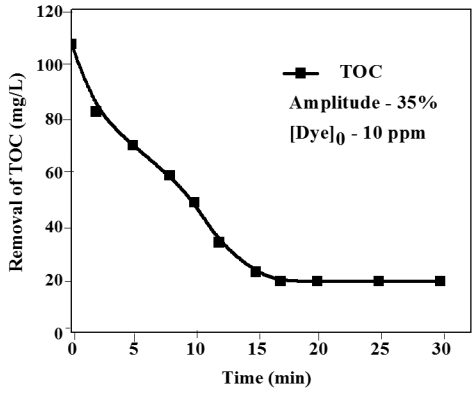

Fig. 15 — Time dependence analysis of TOC level of the degraded DB71dye molecule.

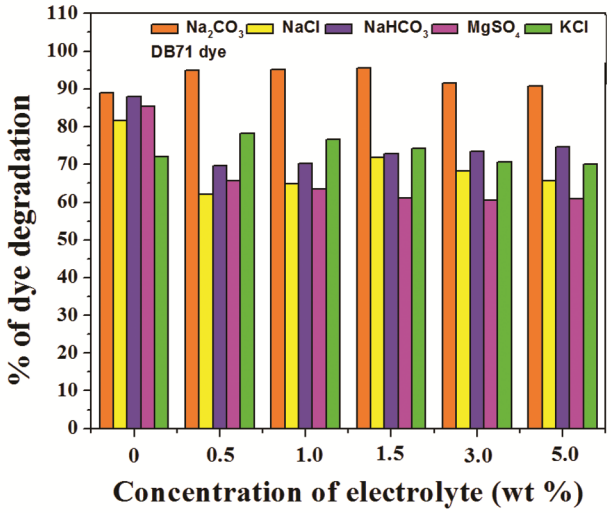

Fig. 16 — Effect of electrolyte concentration on degradation of DB71 dye molecule using ZnONR under ultrasonic irradiation

(1 to 8). When semiconductor catalyst in the aqueous solution was irradiated with US, it undergoes sonolysis of water molecules and also couples with the catalyst to form electron-hole pairs (Equation 6). The electron-hole pairs can produce $OH^{\bullet}$ (eqn7) which can degrade the dye to CO_2, H_2O and inorganic species (Equation 8).

By-product analysis

The formation of by-products during the sonocatalytic degradation of dye molecule with ZnONR under US irradiations were characterized using UV-visible spectrophotometer and ESI-MS analyses. Thus, a plausible degradative reaction mechanism has been proposed.

UV-visible absorption spectroscopy

UV-visible absorption spectrum would usually provide useful evidence on the probable reaction

intermediates and by-products formed during the course of the reaction. The kinetics of dye degradation has been analyzed simultaneously by taking 10 ppm of dye solution at 35% amplitude and recording the UV-visible spectrum from aliquots withdrawn during degradation processes as a function of time was as shown in Fig. 17.

It is specifically determined that the absorption peak at 587 nm (Fig. 17) diminishes rapidly and nearly disappears after 17 min duration of US irradiation. The experimental result clearly indicates that the dye moleculeis completely degraded. The dye degradation has to be confirmed further by ESI-MS analysis of the US irradiated dye sample.

ESI-MS$^+$ analysis

Analysis of by-products present in the sonocatalytically degraded dye samples were carried out by ESI-MS$^+$ technique. The ESI-MS$^+$ spectrum of the neat (Fig. 18(a)) and sonocatalytically degraded samples (Fig. 18(b)) of DB71 dye molecules is given in Fig. 18. The peak observed at m/z 965.15 present in the starting mixture as given in Fig.18(a) which is not present in the degraded intermediates as shown in Fig.18(b). This indicates that the neat dye molecule

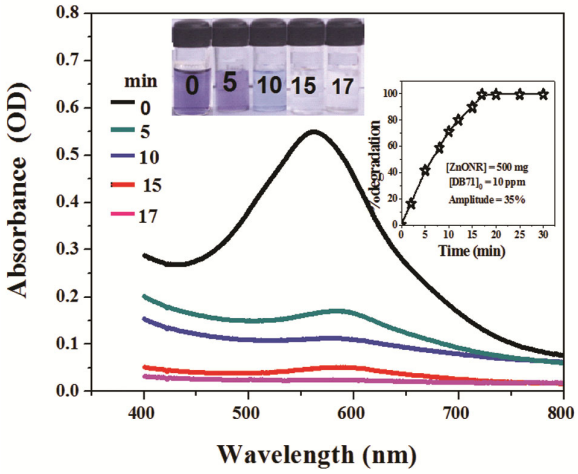

Fig. 17 — UV-Visible absorption spectrum of 10 ppm dye degradation of dye molecule using ZnONR under ultrasonic irradiation (Inset) Kinetics of dye degradation and digital photographs of the degraded sample.

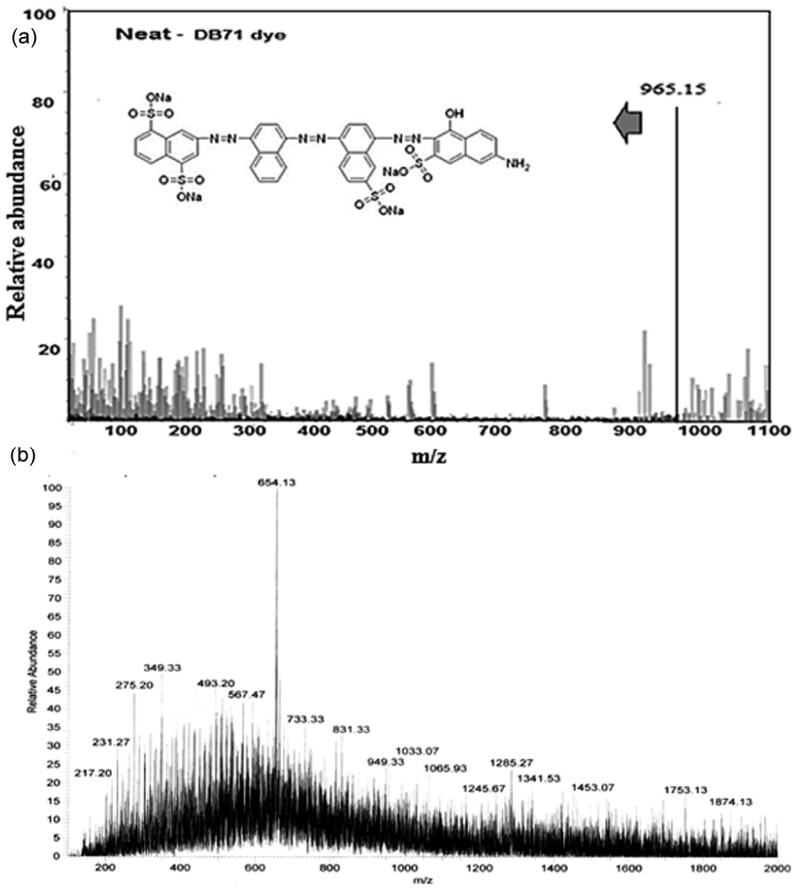

Fig. 18 — ESI-MS$^+$ spectrum of 10 ppm of (a) neat and (b) degraded dye molecule with ZnONR under ultrasonic irradiation.

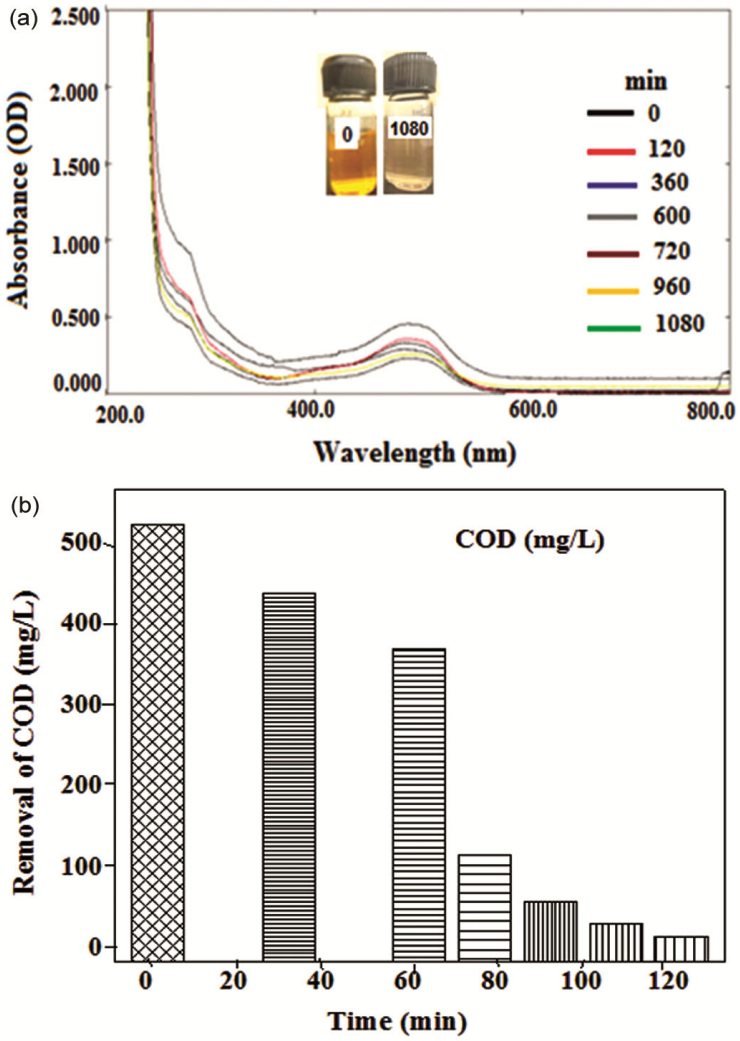

Fig. 19 — (a) UV-Visible absorption spectrum, digital photograph of the neat and degraded dye samples (Inset), and (b) Reduction in COD in mg/L for the real dye house effluent using ZnONR

was degraded and formed fragmented species (m/z 949.33, 831.40, 733.33, 567.47, 493.20, 349.33, 275.20, 231.27, etc).

*A peak at m/z 654.13 is a system peak

Scheme 1 explains the plausible degradative reaction pathway for dye molecule[40].

Reusability test

The reusability of the catalyst was investigated to find out the stability and cost effectiveness of the ZnONR catalyst (Fig.19).

The kinetics experiment was followed by using used ZnONRby following all the parameters constant. Subsequentlyeach cycle, the catalyst was filtered and washed three times with double distilled water and dried at 110°C in an hot air oven. The separated catalyst was then reused for five times by following the same kinetics experiment. This shows that no decrease in catalytic activity in degradation of the dye molecule and no residues, impurities or color change. Thus, this shows that the stability of ZnONR catalyst is better and efficient. For 10 ppm of dye molecule was degraded at 99% in 17 min. This shows that the catalytic action was same even upto the 5 cycles of the reusability.

Sonocatalytic degradation of real dye house effluent

The real dye house effluent collected from Pilot CSIR-CLRI tannery was tested for its degradation efficiency using ZnONR under US irradiations. 1 mL of concentrated dye house effluent was diluted

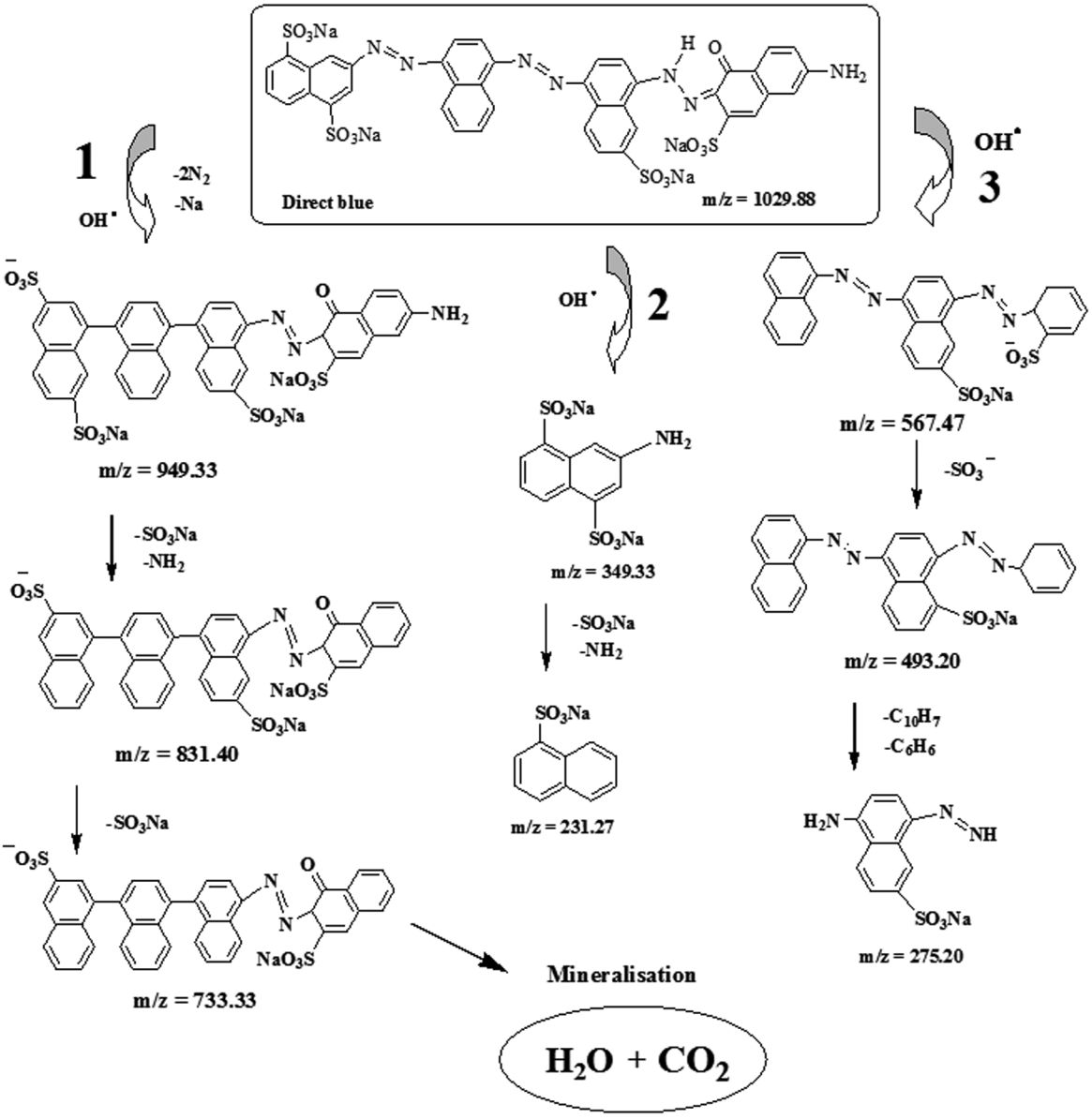

Scheme 1 — Plausible degradative reaction pathway for DB71 dye molecule with ZnONR under ultrasonic irradiation

to 200 ml with optimized dosage of 2 g of ZnONR catalyst and irradiated under ultrasound at 35 % amplitude energy input (Fig. 19 (a)).

Kinetics of dye degradation experiment has been carriedoutto monitor the effect of reaction time on degradation of effluent. Thorough degradation was observed in 1080 min irradiation lead to colourless solution. The peak at 480 nm shows the presence of –C=C- or -N=N- in the effluent. This indicates the peak vanishes during the breakdown of the dye molecules due to the ultrasound assisted catalytic degradation. The reduction of COD as a function of time during the course of the degradation of the effluent is shown in Fig. 19(b). COD removal of 538.46 to 153.85 mg/L was observed in 1080 min US irradiation and 71.43% COD was removed.

Conclusion

ZnO nanorods catalyst was efficiently prepared by precipitation method and the nanorods were characterized by various techniques and its catalytic performances were investigated using DB71dye underultrasound. Complete analysis of the catalyst after sonication was also done. Characterization of the

nanorod is established the nanocrystallinity, elemental composition and surface roughness. The degradation is supposed to be taken place via bubble collapse and hot spot mechanism due to the reactive OH radical production in aqueous phase undersonication. Interference of electrolytes on degradation processes were of lesser impact except that of chloride ions. From the reusability test it is concluded that the catalyst is best appropriate for industrial applications for the degradation studies because, the degradation efficiency was not affected even up to five cycles of kinetic measurements due to the surface cleaning of the catalyst and vigorous agitation of the ultrasound jet. From these studies it was established that complete mineralization of dye may be attained without the formation of toxic by-products.

References

1 Munter R, *Proc Estonian Acad Sci Chem*, 50 (2001) 59.
2 Murugan E & Jebaranjitham J N, *Chem Eng J*, 259 (2015) 266.
3 Santhoshkumar S & Murugan E, *Appl Surf Sci*, 553 (2021) 149544.
4 Glaze W H, Kang, J W & Chapin D H, *Ozone Sci Eng*, 9 (1987) 335.
5 Fenton H J H, *J Chem Soc Tran*, 65 (1894) 899.
6 Herra F, Kiwi J, Lopez A & Nadtochenko V, *Environ Sci Technol*, 33 (1999) 3145.
7 Ikehata K, Jodeiri Naghashkar N & Gamal El-Din M, *Ozone Sci Eng*, 28 (2006) 353.
8 Wang J, Jiang Z, Zhang Z, Xie Y, Lv Y, Li J, Deng Y & Zhang X, *Sep Purif Technol*, 67 (2009) 38.
9 Pang Y L, Abdullah A Z & Bhatia S, *J Appl Sci*, 10 (2010) 1068.
10 Rodriguez E M, Fernandez G & Alvarez P M, *App Cat B Environ*, 102 (2011) 572.
11 Mathur N, Bhatnagar P, Naga P & Bijarnia M K, *Ecotox Environ Safe*, 61 (2005) 105.
12 Gaunt I F, Wright M & Grasso P, *Toxicology*, 9 **(**1971) 329.
13 Murugan E, Santhoshkumar S, Reshna K M & Govindaraji S, *J Mater Sci*, 54 (2019) 5294.
14 Murugan E & Rangasamy R, *J Biomed Nanotech*, 7 (2011) 225.
15 He Z, Song S, Zhou H, Ying H J & Chen C I, *Ultrason Sono Chem*, 14 (2007) 298.
16 Wang J, Ma T, Zhang Z, Zhang X, Jiang Y, Dong D, Zhang P & Li Y, *J Hazard Mater*, 137 (2006) 972.
17 Gao J, Liu B, Wang J, Jin X, Jiang R, Liu L, Wang B & Xu Y, *Spectrochim Acta Mol Biomolspectrosc*, 77 (2010) 895.
18 Jung H & Choi H, *J Appl Catal B-Environ*, 66 (2006) 288.
19 Zuas O, Budiman H & Hamim N, *Adv Mat Lett*, 4 (2013) 662.
20 Shanmugam P, Rajakumar K, Boddula R, Renathung C, Ngullie Wei W, Xie J & Murugan E, *J Mater Sci Technol*, 2 (2019) 532.
21 Johar A, Afzal R A, Alazba A A & Manzoor U, *Adv Mater Sci Eng*, 2015 (2015) 1.
22 Wang J, Jiang Z, Zhang Z, Xie Y, Wang X, Xing Z, Xu R & Zhang X, *Ultrason Sonochem*, 15 (2008) 768.
23 Limin S, Yamiao L, Peizhi H, Shujuan Z, Xiaoqing W, Sheng F, Juanjuan S & Donglan S, *Ultrason Sonochem*, 21 (2014) 1318.
24 Murugan E & Shanmugam P, *J Nano Sci Nanotech*, 16 (2016) 426.
25 Nepiras E A, *Ultrasonics*, 22 (1984) 25.
26 Flint E B & Suslick K S, *Science*, 253 (1991)1397.
27 Bang J H & Suslick K S, *Adv Mater*, 22 (2010) 1039.
28 Ince N H, Tezcanli G, Belen R K & Apikyan I G, *Appl Catal B-Environ*, 29 (2001) 167.
29 Eskandarloo H, Badiei A, Behnajady M A & Ziarani G M, *Ultrason Sonochem*, 28 (2016) 169.
30 Ogi H, Hirao M & Shimoyama M, *Ultrasonics*, 40 (2002) 649.
31 Biglari H, Javan N, Khosravi R & Zarei A, *Iran J Health Sci*, 4 (2016) 55.
32 Buettner G R & Oberley L W, *Biochem Biophy Res Commun*, 3 (1978) 69.
33 Yue H Y, Fei W D, Li Z J & Wang L D, *J Sol-Gel Sci Technol*, 44 (2007) 259.
34 Liu Z, Deng J & Li F, *Mater Sci Eng B*, 150 (2008) 99.
35 Jenkins R V & Snyder R L, 138 (1996) 391.
36 Georgiou D, Melidis P, Aivasidis A & Gimouhopoulos K, *Dyes Pigm*, 52 (2002) 69.
37 Neppolian B, Choi H C, Sakthivel S, Arabindoo B & Murugesan V, *Hazard Mater*, 89 (2002) 303.
38 Sauer T, Neto G C, Jose H J & Moreira R F P M, *J Photochem Photobiol A Chem*, 149 (2002) 147.
39 Shanthi M & Kuzhalosai V, *Indian J Chem*, 51 (2012) 428.
40 Ali L, Algaithi R, Habib H M, Souka U, Rauf M A & Ashraf S S, *BMC Biochem*, 14 (2013) 1.